IEEE Access
Multidisciplinary | Rapid Review | Open Access Journal

Received August 27, 2018, accepted September 22, 2018, date of publication October 5, 2018, date of current version November 9, 2018.

Digital Object Identifier 10.1109/ACCESS.2018.2873580

Design of a Hemispherical Reconfigurable Frequency Selective Surface Using Water Channels

DONG-CHAN SON[1], HOKEUN SHIN[1], YOON JAE KIM[2], IC PYO HONG[3], HEOUNG JAE CHUN[4], KYUNG-YOUNG JUNG[5], HOSUNG CHOO[6], AND YONG BAE PARK[1], (Senior Member, IEEE)

[1]Department of Electrical and Computer Engineering, Ajou University, Suwon 16499, South Korea
[2]Agency for Defense Development, Daejeon 34186, South Korea
[3]Department of Information & Communication Engineering, Kongju National University, Cheonan 31080, South Korea
[4]School of Mechanical Engineering, Yonsei University, Seoul 03722, South Korea
[5]Department of Electronic Engineering, Hanyang University, Seoul 04763, South Korea
[6]School of Electronic and Electrical Engineering, Hongik University, Seoul 04066, South Korea

Corresponding author: Yong Bae Park (yong@ajou.ac.kr)

This work was supported in part by the Low Observable Technology Research Center Program of Defense Acquisition Program Administration and Agency for Defense Development, in part by the Basic Science Research Program through the National Research Foundation of Korea (NRF) through the Ministry of Science and ICT under Grant 2017R1A2B4001903, and in part by the Basic Science Research Program through the National Research Foundation of Korea (NRF) funded by the Ministry of Education under Grant 2015R1A6A1A0303 1833.

ABSTRACT In this paper, we propose a hemispherical reconfigurable frequency selective surface (FSS) using water channels. The switching between band-pass and band-stop states is possible since the water with a high dielectric constant can control the effective permittivity of the structure. We simulate and fabricate the FSS and measure the radiation pattern of FSS enclosed horn antenna to check the reconfigurable characteristic of the hemispherical FSS. The simulated results show a good agreement with the measured results.

INDEX TERMS Frequency selective surface, hemisphere radomes, water channels.

I. INTRODUCTION

Frequency selective surface (FSS) is a periodic structure which can selectively transmit or reflect electromagnetic (EM) waves at specific frequencies. FSSs have been widely used as a filter in radomes, antennas, reflectors, absorbers, and so on. Conventional passive FSSs have the disadvantage of merely operating at a fixed single designed frequency, which limits their use in practical applications. To overcome this drawback, reconfigurable FSS has been extensively studied using various methods, including circuit tuning and material tuning methods. Circuit tuning methods often use active elements, such as PIN diodes, varactor diodes, and micro-electromechanical systems (MEMS) [1]–[11], while the material tuning methods employ liquid crystals, ferrite substrates, and graphenes [12]–[20]. The FSS structure using PIN diodes realizes the frequency reconfigurable function by controlling the bias voltage (on-off state) applied to the PIN diodes [1], [2]. Number and location of the PIN diodes in a unit cell have a significant effect on the performance of the FSS. It has the advantages of a wide variable range of the transmission frequency and low loss. However, there are disadvantages such as only two variable transmission frequencies, slow switching time, and difficulty in accurate fabrication due to nonlinearity [3], [4]. The FSS structure using varactor diodes realizes the frequency reconfigurable function by adjusting the diode capacitance according to the applied bias voltage [5]–[7]. This not only produces more transmission frequencies, but also has low loss and faster switching time [8]. However, it is difficult to operate in the high frequency band and the manufacturing cost is relatively high [9]. The FSS structure using MEMS realizes the frequency reconfigurable function by controlling capacitance of the system [10], [11]. It has the advantages of reduced manufacturing cost, low loss, high isolation, and fast switching [12]. However, since the size of the MEMS elements is too small, the transmission frequency bandwidth is narrow and the change range of capacitance is small [12], [13]. The FSS applying the bias voltage to the liquid crystal changes its orientation of the molecule that causes a change in the

dielectric constant and the FSS frequency response [14]. It has the advantage of a tunable capability over a wide frequency range, but has the disadvantage of difficulty in realization due to the complicated structure [15]. The magnetically tunable FSS is implemented by using a ferrite substrate, where the permeability of the ferrite substrate can vary with the external bias magnetic field. This has advantages that the magnetically tunable FSSs do not need a bias circuit, but it often suffers from several disadvantages, such as low tuning speed and narrow tuning range [16]. Graphene has been considered as a good candidate for designing tunable FSSs, as it possesses extraordinary properties over a wide-band frequency range, such as high mobility, large thermal conductivity, and strong intrinsic strength, come from the special atomic structures [17], [18]. But realizing such a material is challenging due to difficulty in controlling the surface conductivity [19], [20]. Recently, the method using the fluidic channel to obtain the reconfigurable properties has been studied extensively [21]–[23]. The FSS using fluidic channels has the ability, such as drastic change of electrical characteristics, a variety of designs using various parameters and wide tuning ranges. Therefore, fluidic channels can be suitable for use in a reconfigurable FSS realization. We also have proposed the reconfigurable FSS using the fluidic channels in planar dielectric slab [24]. However, since we have only confirmed the reconfigurability of the planar structure, it could not guarantee the feasibility of the practical structures such as radomes.

In this letter, we propose a hemispherical reconfigurable FSS using water channels. The switching between band-pass and band-stop states is possible since water with a high dielectric constant ($\varepsilon_r = (66 \sim 57) - j(26 \sim 33)$, when the frequency is from 8 GHz to 12.5 GHz at 25 degrees Celsius) [25] can control the effective permittivity of the structure. The relative permittivity (ε_r) of a material is its permittivity expressed as a ratio relative to the permittivity of a vacuum. The detailed dimensions of the FSS such as a diameter and number of tubes are optimized using a full-wave EM simulation software (CST MICROWAVE STUDIO (MWS) [26]). To check the reconfigurable characteristic of the hemispherical FSS, we then fabricate the optimized FSS and measure the radiation pattern when a horn antenna is placed inside the FSS. The simulated results show a good agreement with the measurement, which confirms that the proposed FSS can be suitable for use in a reconfigurable FSS.

II. DESIGN AND FABRICATION

Fig. 1 shows the design procedure for reconfigurable structures. First, we have figured out transmission characteristics of planar dielectric slab without fluidic channels by changing parameters such as permittivity and thickness. We have compared the simulation results with calculated results using equation (1) (see Fig. 2) to obtain the reliability of the simulation results for the simplest planar structure which the fluidic channels are not inserted. Fig. 3 illustrates that the

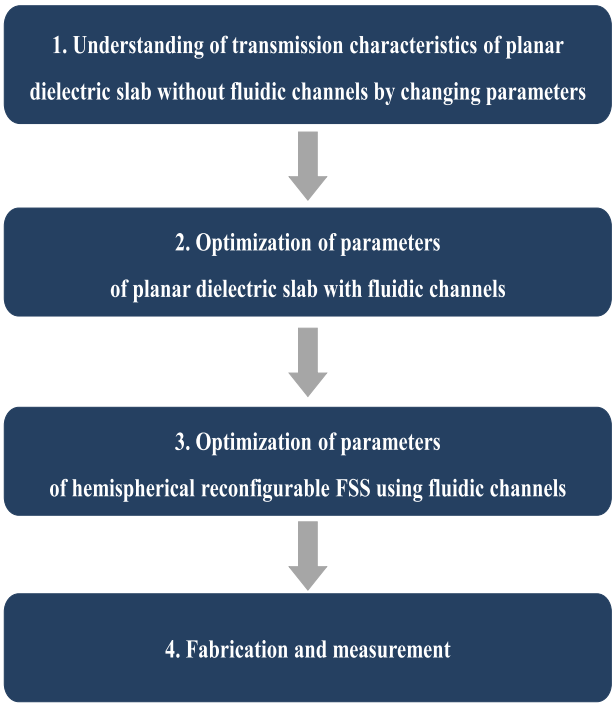

FIGURE 1. Design procedure for reconfigurable structures.

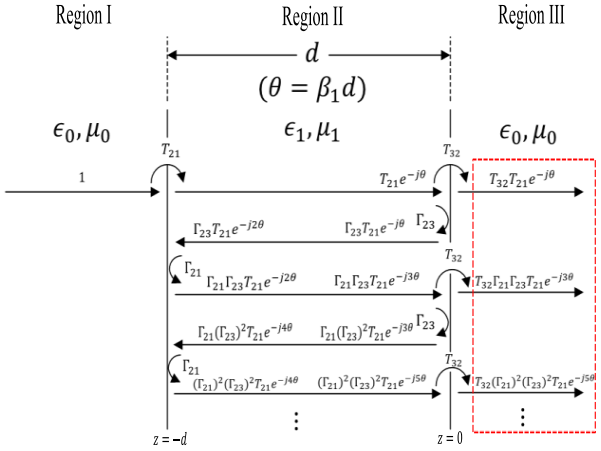

FIGURE 2. Transmission coefficient of wave passing through dielectric slab.

thickness of the dielectric slab can change only the frequency interval between the maximum and minimum values of the transmission coefficient when the real part (ε': eps1) of permittivity is 5 and imaginary part (ε'': eps2) of permittivity is zero. Also, to understand the effects of real part (eps1) and imaginary part (eps2) of the permittivity of the dielectric slab (100 mm × 100 mm × 10 mm) on the transmission characteristic, the transmission coefficients are calculated in terms of the permittivity of the dielectric slab. Fig. 4 shows the transmission coefficients in terms of eps1 when eps2 is zero. This indicates that the difference between the minimum and the maximum transmission coefficients increases as a

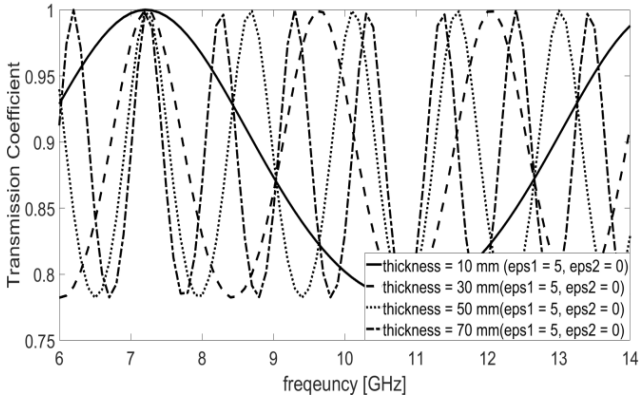

FIGURE 3. Transmission coefficients according to the thickness of dielectric slab.

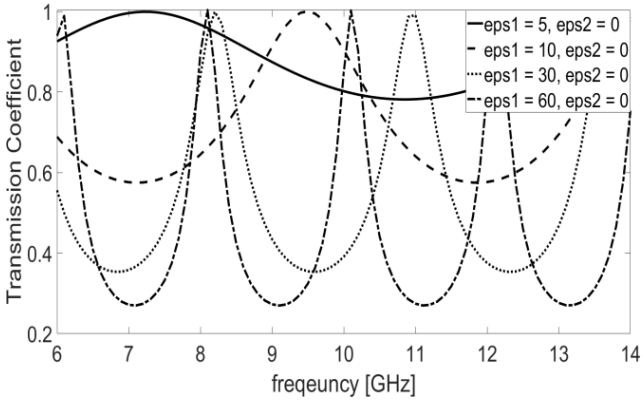

FIGURE 4. Transmission coefficients according to eps1.

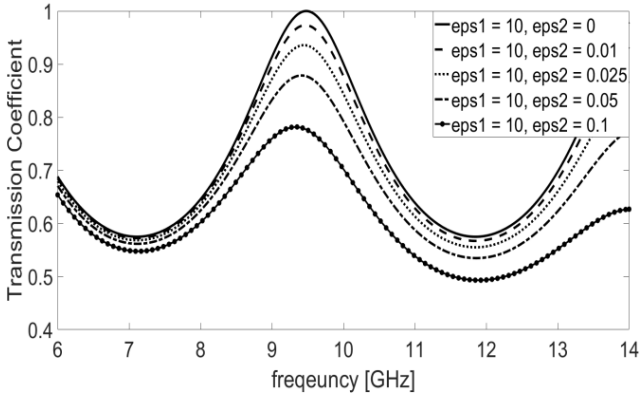

FIGURE 5. Transmission coefficients according to eps2.

real part (eps1) of the permittivity increases. The real part of the permittivity can also change periods between the maximum and minimum values of the transmission coefficient. Fig. 5 illustrates the transmission coefficients in terms of eps2 when eps1 is 10. It is seen that the imaginary part of the permittivity only affects attenuation. Next, the spacing and thickness of tubes of the dielectric slab inserted fluidic channels are optimized using CST MWS [24]. Third, we have optimized parameters such as number and diameter of channels

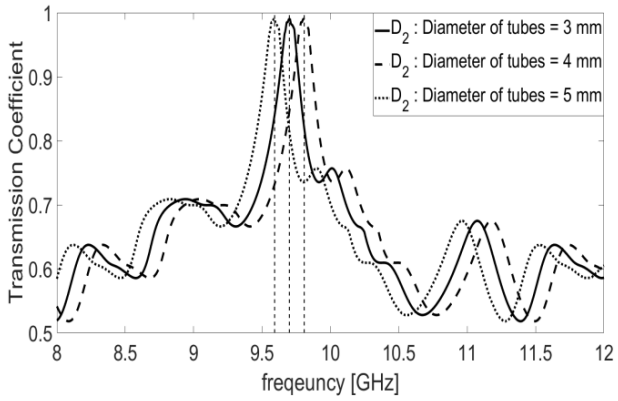

FIGURE 6. Transmission coefficient depending on the diameter of tubes.

of hemispherical reconfigurable FSS for a target frequency. Finally, we have fabricated and measured the structure to check the validity of our design. Fig. 7 shows the procedure for verifying the feasibility of the hemispherical reconfigurable FSS with water channels. First, we should determine a specific configuration among practical structures. Since the hemispherical structure has a constant curvature for any directions from the vertex, we can easily insert the water channels in implementing the

$$
\begin{aligned}
&T(z=0^{+}) \\
&\quad = \frac{T_{32}T_{21}e^{-j\theta}}{1-\Gamma_{21}\Gamma_{23}e^{-j2\theta}} \\
&T_{32} = \frac{2\times\eta_{regionIII}}{\eta_{regionIII}+\eta_{regionII}}, \quad T_{21} = \frac{2\times\eta_{regionII}}{\eta_{regionI}+\eta_{regionII}}, \\
&\Gamma_{21} = \frac{\eta_{regionI}-\eta_{regionII}}{\eta_{regionII}+\eta_{regionI}}, \quad \Gamma_{23} = \frac{\eta_{regionIII}-\eta_{regionII}}{\eta_{regionIII}+\eta_{regionII}}
\end{aligned} \tag{1}
$$

FSS. Therefore, we have selected the hemispherical FSS. We also find its application in hemisphere radomes. Second, it is necessary to find an insertion structure of fluidic channels that can significantly change the effective permittivity of the structure while achieving structural stability and feasibility. So, we decided to insert fluidic channels similar to the frame structure of an umbrella. Third, to design the reconfigurable FSS operating at 9.7 GHz, we have optimized the dimensions of the FSS by changing the diameter and number of tubes using a full-wave solver. We have obtained simulation results by changing the diameter (D_2) and number (N_1) of tubes (see Fig. 6 and 8). When the number and diameter of the tubes are changed, the center frequency is also shifted. However, it can be seen that the diameter of the tube does not significantly change the transmission characteristics. The effective permittivity of the structure can be changed by varying diameter and number of tubes to obtain the reconfigurable characteristic in the X-band. Fourth, the design structure is fabricated and measured in an anechoic chamber. Finally, we compare simulation results with measurement results.

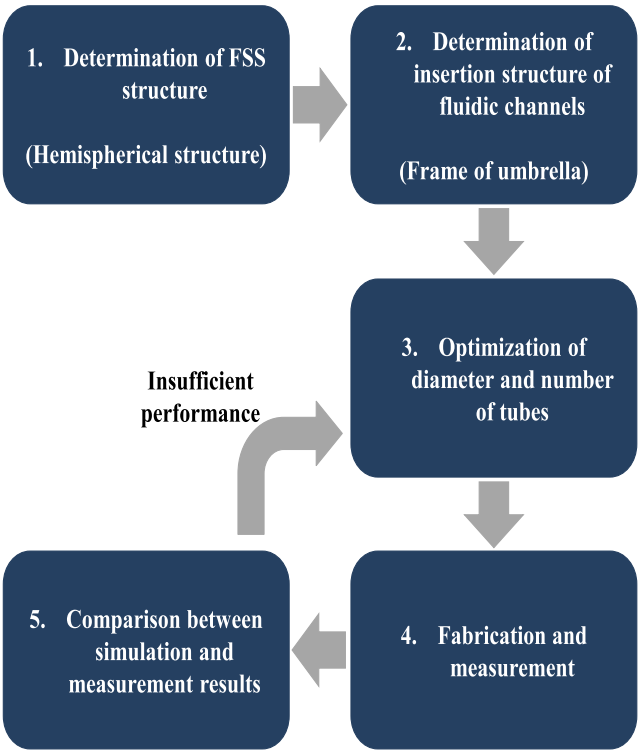

FIGURE 7. Design procedure to verifying feasibility of hemispherical structure.

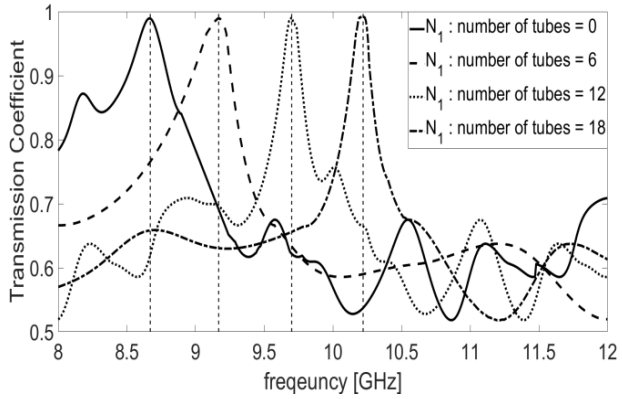

FIGURE 8. Transmission coefficient depending on the number of tubes.

TABLE 1. Design parameters of hemispherical reconfigurable FSS for operating at target frequency.

Parameter	Value
D_1 : Diameter of radome (mm)	300
D_2 : Diameter of tubes (mm)	4
t_1 : Tube thickness (mm)	0.5
t_2 : Foam thickness (mm)	6.5
t_3 : Composite thickness (mm)	1.125
t_4 : Adhesive thickness (mm)	0.02
N_1: Number of tubes	12

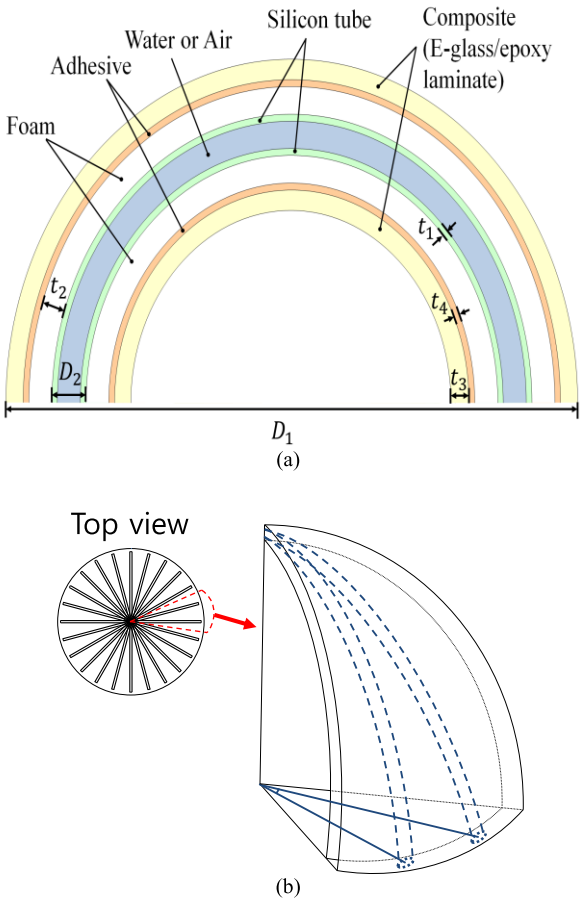

FIGURE 9. Geometry of the hemispherical reconfigurable FSS: (a) Cross section view; (b) Perspective view.

If the performance of results has not served what we have established, we should go back to step 3 to solve the problem. The optimized the design parameters are listed in Table 1. Fig. 9 shows the reconfigurable FSS for a real hemisphere radome, which consists of foam (Rohacell HF- 71), composites (E-glass/epoxy laminate), adhesives, and silicon tubes that can be filled or unfilled with water. The foam is carved with designed dimensions, and the holes are extracted from the foam. To make the curvature, thermal-forming process is performed. The channel made of silicon is then inserted in the holes, which can be filled or unfilled with water. Finally, the adhesive is applied to the curved-foam and the composites are attached on the outside and inside of the foam to achieve mechanical strength, harness, and stability. The fabricated hemispherical FSS with metric is shown in Fig. 10. Fig. 11(a) is the 3-D model in the simulation. Fig. 11(b)-(f) have shown that the transmission coefficients, reflection coefficients, phase responses and radiation patterns between the filled state and the unfilled state are varied. The difference in the transmission coefficient is about 0.4 (i.e., the difference in power is 64 %) and the difference in the radiation patterns with phi $= 0°$ is about 5 dB at 9.7 and 8.7 GHz. Note that the structure filled with water at 9.7 GHz has a band-pass characteristic, whereas the structure without water at 8.7 GHz has a band-pass characteristic. There is little

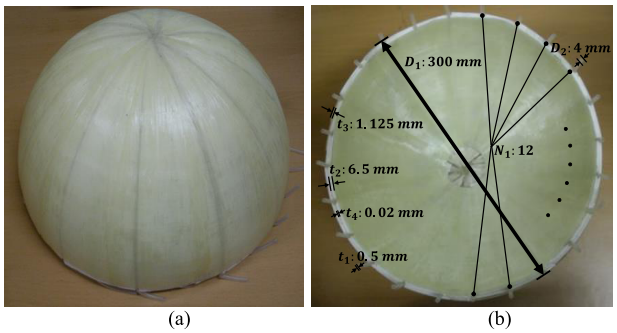

FIGURE 10. Fabricated hemispherical reconfigurable FSS: (a) Top view; (b) Bottom view.

difference between water filled and water unfilled at 10.8 GHz. As a result, we can obtain the reconfigurable characteristic using water channels. In addition, we should consider the effect of the water since the water has a high dielectric constant. In the designed structure, the loss of water is very small due to the small size of the tube with the diameter of about 0.1λ. In other words, EM waves hardly attenuate in our FSS structure when they pass through the water. By confirming the results of transmission coefficient and radiation patterns, we can conclude that the hemispherical reconfigurable FSS capable of transmitting EM waves at a specific frequency can be implemented by using the water channels.

III. MEASUREMENT

In order to verify the transmission characteristics of the fabricated structure, a measurement setup using an indoor anechoic chamber is utilized as illustrated in Fig. 12. This measurement system includes two horn antennas (ANT-SGH-90, gain : 22 dB, frequency : 8.2-12.4 GHz) serving as a transmitting and receiving antennas. Inner surfaces of the anechoic chamber are covered with pyramidal absorbers to minimize interference from reflection and external noise. While the hemispherical FSS is illuminated from the transmitting antenna, the FSS with the receiving antenna is rotated, and the received power is recorded for each rotation angle. Figs. 13(a) and 13(b) show the measured and simulated radiation patterns of the proposed FSS at 8.7 GHz and 9.7 GHz, respectively. Note that the structure filled with water at 9.7 GHz has a band-pass characteristic, whereas the structure without water at 8.7 GHz has a band-pass characteristic (See Fig. 11(b)). The comparison between the measurement and simulation results shows a good agreement. When the FSS is used in the band-pass state at 8.7 GHz and 9.7 GHz, only signals within the desired band can be completely received. On the other hand, in the band-stop state, signals are effectively reflected by the FSS. Therefore, it is confirmed that the desired reconfigurable characteristic at the target frequency can be achieved by configuring the hemispherical FSS with water channels. Fig. 13(c) shows that the comparison between water filled and water unfilled shows a good agreement since

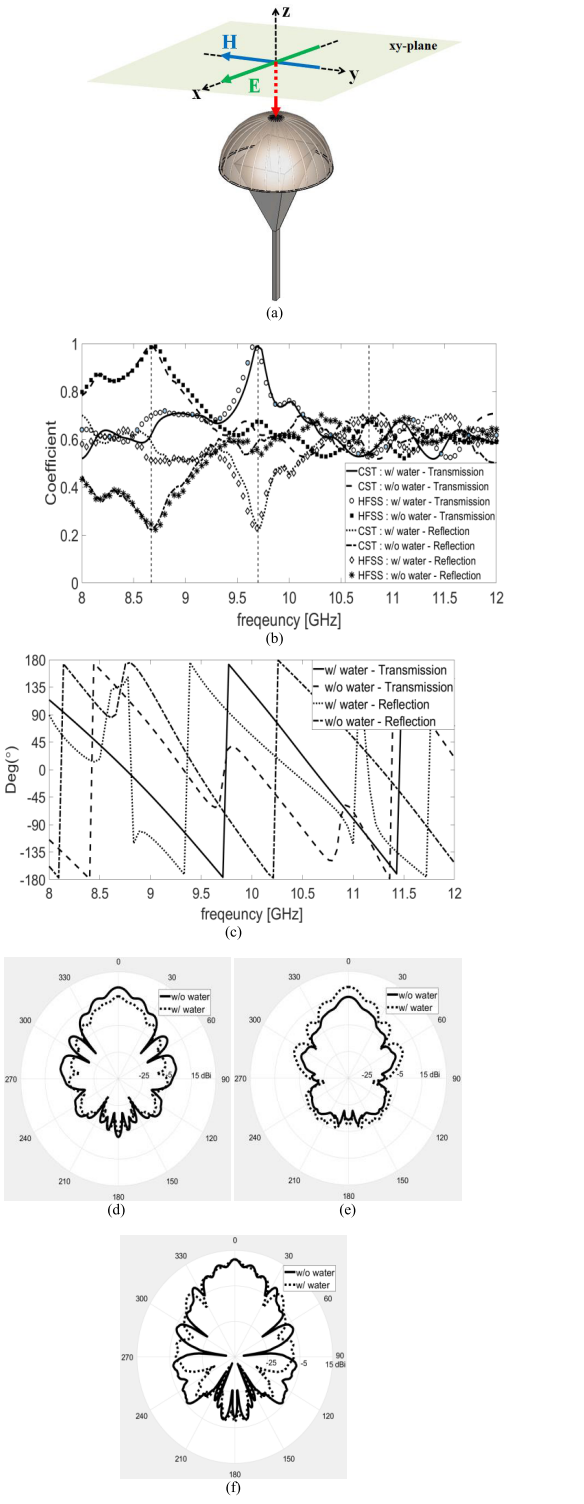

FIGURE 11. 3-D model and the simulated results of the hemispherical reconfigurable FSS: (a) Simulation geometry; (b) Simulation result of CST MWS and ANSYS HFSS; (c) Phase responses; (d) radiation pattern at 8.7GHz; (e) Radiation pattern at 9.7 GHz; (f) Radiation pattern at 10.8 GHz.

there is little difference between transmission coefficients of two cases at 10.8 GHz (See Fig. 11(b)).

Our system works by manually inserting or draining water into the channel. Fast-state-switching-speed requires

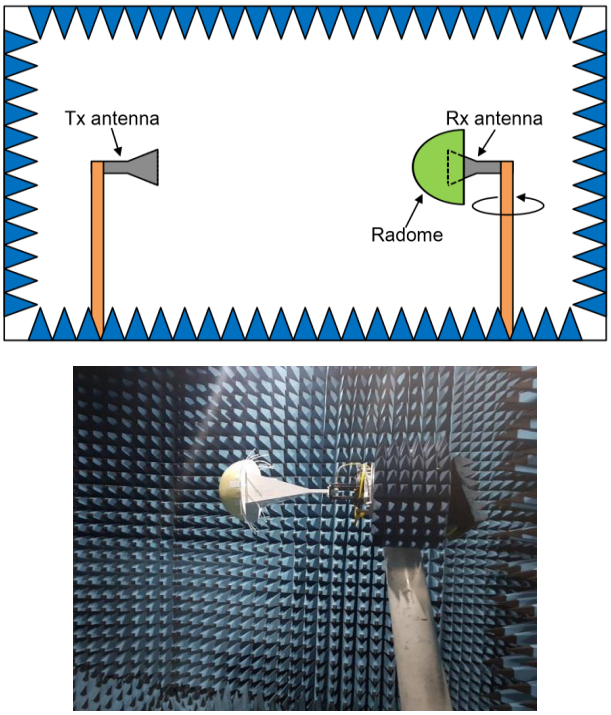

FIGURE 12. Measurement setup.

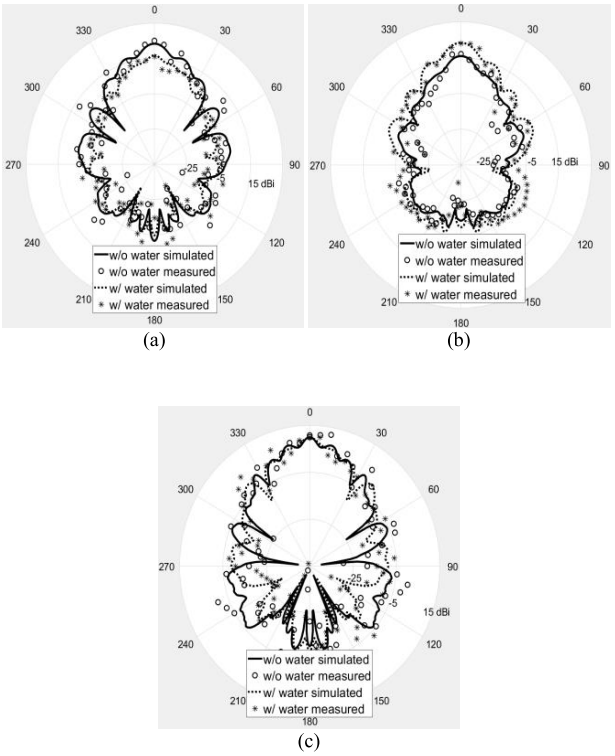

FIGURE 13. Comparison between measured and simulated radiation patterns of the hemispherical reconfigurable FSS: (a) 8.7 GHz; (b) 9.7 GHz; (c) 10.8 GHz.

automation of water pumping and draining systems. This study is limited to examine the feasibility of a hemispherical reconfigurable FSS using water channels, and further research is needed to implement a practical system in the future.

IV. CONCLUSION

We have designed, fabricated, and measured a hemispherical reconfigurable FSS using water channels in the X-band. It has been demonstrated that the effective permittivity of the hemispherical structure can be changed by varying the radius and number of tubes. Our results demonstrated the reconfigurability of FSS using fluidic channels, which can be used in practical applications of reconfigurable FSS radomes.

REFERENCES

[1] D. Peroulis, K. Sarabandi, and L. P. B. Katehi, "Design of reconfigurable slot antennas," *IEEE Trans. Antennas Propag.*, vol. 53, no. 2, pp. 645–654, Feb. 2005.

[2] M. Niroo-Jazi and T. A. Denidni, "Electronically sweeping-beam antenna using a new cylindrical frequency-selective surface," *IEEE Trans. Antennas Propag.*, vol. 61, no. 2, pp. 666–676, Feb. 2013.

[3] G. I. Kiani, K. L. Ford, L. G. Olsson, K. P. Esselle, and C. J. Panagamuwa, "Switchable frequency selective surface for reconfigurable electromagnetic architecture of buildings," *IEEE Trans. Antennas Propag.*, vol. 58, no. 2, pp. 581–584, Feb. 2010.

[4] Y.-Y. Lin, C.-L. Liao, T.-H. Hsieh, and W.-J. Liao, "A novel beam-switching array antenna using series-fed slots with PIN diodes," *IEEE Antennas Wireless Propag. Lett.*, vol. 16, pp. 1393–1396, Dec. 2016.

[5] F. Costa, A. Monorchio, and G. P. Vastante, "Tunable high-impedance surface with a reduced number of varactors," *IEEE Antennas Wireless Propag. Lett.*, vol. 10, pp. 11–13, Mar. 2011.

[6] A. Ebrahimi, Z. Shen, W. Withayachumnankul, S. F. Al-Sarawi, and D. Abbott, "Varactor-tunable second-order bandpass frequency-selective surface with embedded bias network," *IEEE Trans. Antennas Propag.*, vol. 64, no. 5, pp. 1672–1680, May 2016.

[7] L. Zhang, Q. Wu, and T. A. Denidni, "Electronically radiation pattern steerable antennas using active frequency selective surfaces," *IEEE Trans. Antennas Propag.*, vol. 61, no. 12, pp. 6000–6007, Dec. 2013.

[8] A. Boukarkar, X. Q. Lin, and Y. Jiang, "A dual-band frequency-tunable magnetic dipole antenna for WiMAX/WLAN applications," *IEEE Antennas Wireless Propag. Lett.*, vol. 15, pp. 492–495, Mar. 2016.

[9] Y. Wang, K.-C. Yoon, and J.-C. Lee, "A frequency tunable double band-stop resonator with voltage control by varactor diodes," *J. Electromagn. Eng. Sci.*, vol. 16, no. 3, pp. 159–163 Jul. 2016.

[10] M. Safari, C. Shafai, and L. Shafai, "X-band tunable frequency selective surface using MEMS capacitive loads," *IEEE Trans. Antennas Propag.*, vol. 63, no. 3, pp. 1014–1021, Mar. 2015.

[11] K. M. J. Ho and G. M. Rebeiz, "A 0.9–1.5 GHz microstrip antenna with full polarization diversity and frequency agility," *IEEE Trans. Antennas Propag.*, vol. 62, no. 5, pp. 2398–2406, May 2014.

[12] J. M. Zendejas, J. P. Gianvittorio, Y. Rahmat-Samii, and J. W. Judy, "Magnetic MEMS reconfigurable frequency-selective surfaces," *J. Microelectromech. Syst.*, vol. 15, no. 3, pp. 613–623, Jun. 2006.

[13] N. Kumar and Y. K. Singh, "RF-MEMS-based bandpass-to-bandstop switchable single- and dual-band filters with variable FBW and reconfigurable selectivity," *IEEE Trans. Microw. Theory Techn.*, vol. 65, no. 10, pp. 3824–3837, Oct. 2017.

[14] W. Hu *et al.*, "Liquid crystal tunable mm wave frequency selective surface," *IEEE Microw. Wireless Compon. Lett.*, vol. 17, no. 9, pp. 667–669, Sep. 2007.

[15] E. Doumanis *et al.*, "Electronically reconfigurable liquid crystal based mm-wave polarization converter," *IEEE Trans. Antennas Propag.*, vol. 62, no. 4, pp. 2302–2307, Apr. 2014.

[16] T. K. Chang, R. J. Langley, and E. A. Parker, "Frequency selective surfaces on biased ferrite substrates," *Electron. Lett.*, vol. 30, no. 15, pp. 1193–1194, Jul. 1994.

[17] E. Carrasco and J. Perruisseau-Carrier, "Reflectarray antenna at terahertz using graphene," *IEEE Antennas Wireless Propag. Lett.*, vol. 12, pp. 253–256, Feb. 2013.

[18] X. Li, L. Lin, L.-S. Wu, W.-Y. Yin, and J.-F. Mao, "A bandpass graphene frequency selective surface with tunable polarization rotation for THz applications," *IEEE Trans. Antennas Propag.*, vol. 65, no. 2, pp. 662–672, Feb. 2017.
[19] J. Chen, G. Hao, and Q.-H. Liu, "Using the ADI-FDTD method to simulate graphene-based FSS at terahertz frequency," *IEEE Trans. Electromagn. Compat.*, vol. 59, no. 4, pp. 1218–1223, Aug. 2017.
[20] X. Huang, X. Zhang, Z. Hu, M. Aqeeli, and A. Alburaikan, "Design of broadband and tunable terahertz absorbers based on graphene metasurface: Equivalent circuit model approach," *IET Microw., Antennas Propag.*, vol. 9, no. 4, pp. 307–312, Aug. 2015.
[21] A. J. King, J. F. Patrick, N. R. Sottos, S. R. White, G. H. Huff, and J. T. Bernhard, "Microfluidically switched frequency-reconfigurable slot antennas," *IEEE Antennas Wireless Propag. Lett.*, vol. 12, pp. 828–832, Jun. 2013.
[22] M. Konca and P. A. Warr, "A frequency-reconfigurable antenna architecture using dielectric fluids," *IEEE Trans. Antennas Propag.*, vol. 63, no. 12, pp. 5280–5286, Dec. 2015.
[23] C. Borda-Fortuny, K.-F. Tong, A. Al-Armaghany, and K.-K. Wong, "A low-cost fluid switch for frequency-reconfigurable vivaldi antenna," *IEEE Antennas Wireless Propag. Lett.*, vol. 16, pp. 3151–3154, Nov. 2017.
[24] D. C. Son, H. Shin, Y. J. Kim, I. P. Hong, H. J. Chun, and Y. B. Park, "Design and fabrication of a reconfigurable frequency selective surface using fluidic channels," *J. Elect. Eng. Technol.*, vol. 12, no. 6, pp. 2342–2347, Nov. 2017.
[25] M. Kouzai, A. Nishikata, K. Fukunaga, and S. Miyaoka, "Complex permittivity measurement at millimetre-wave frequencies during the fermentation process of Japanese sake," *J. Phys. D, Appl. Phys.*, vol. 40, pp. 54–60, Dec. 2006.
[26] (2014). *CST Microwave Studio*. [Online]. Available: https://www.cst.com/

DONG-CHAN SON received the B.S. degree from the Department of Electrical and Computer Engineering, Ajou University, Suwon, South Korea, in 2017, where he is currently pursuing the M.S. degree. His research interests include electromagnetic field analysis and frequency selective surfaces.

HOKEUN SHIN received the B.S. degree in electrical and computer engineering from Ajou University, Suwon, South Korea, in 2015, where he is currently pursuing the M.S. and Ph.D. degrees with the Department of Electrical and Computer Engineering. His research interests include radomes and radar cross section.

YOON JAE KIM received the Ph.D. degree in mechanical engineering from Seoul National University, Seoul, South Korea, in 2011. From 2011 to 2012, he was a Senior Researcher with the Institute of Advance Machines and Design, Seoul National University, Seoul. In 2012, he joined the Agency for Defense Development, Deajeon, South Korea. His research includes optimal design of composite structures and frequency selective radomes.

IC PYO HONG received the B.S., M.S., and Ph.D. degrees in electronics engineering from Yonsei University, Seoul, South Korea, in 1994, 1996, and 2000, respectively. From 2000 to 2003, he was with the Information and Communication Division, Samsung Electronics Company, Suwon, South Korea, where he was a Senior Engineer with CDMA Mobile Research. Since 2003, he has been with the Department of Information and Communication Engineering, Kongju National University, Cheonan, South Korea, where he is currently a Professor. In 2006 and 2012, he was a Visiting Scholar with the Texas A&M University, College Station, TX, USA, and Syracuse University, Syracuse, NY, USA, respectively. His research interests include numerical techniques in electromagnetics and periodic electromagnetic structures.

HEOUNG JAE CHUN received the B.S. and M.S. degrees in mechanical engineering from Yonsei University, Seoul, South Korea, in 1986 and 1988, respectively, and the Ph.D. degree in mechanical engineering from Northwestern University, Evanston, USA, in 1994.

From 1990 to 1994, he was a Research Assistant with the Center for Quality Engineering and Failure Prevention, Northwestern University. From 1994 to 1997, he was a Post-Doctoral Research Associate with Quality Engineering and Failure Prevention, Northwestern University.

In 1997, he joined the School of Mechanical Engineering, Yonsei University, where he is currently a Professor. His research interests include analysis and design of composite structures.

KYUNG-YOUNG JUNG received the B.S. and M.S. degrees in electrical engineering from Hanyang University, Seoul, South Korea, in 1996 and 1998, respectively, and the Ph.D. degree in electrical and computer engineering from The Ohio State University, Columbus, OH, USA, in 2008. From 2008 to 2009, he was a Post-Doctoral Researcher with The Ohio State University, and from 2009 to 2010, he was an Assistant Professor with the Department of Electrical and Computer Engineering, Ajou University, South Korea. Since 2011, he has been with Hanyang University, where he is currently an Associate Professor with the Department of Electronic Engineering. His current research interests include computational electromagnetics, bio electromagnetics, and nano electromagnetics.

HOSUNG CHOO received the B.S. degree in radio science and engineering from Hanyang University, Seoul, in 1998, and the M.S. and Ph.D. degrees in electrical and computer engineering from The University of Texas at Austin in 2000 and 2003, respectively. In 2003, he joined the School of Electronic and Electrical Engineering, Hongik University, Seoul, South Korea, where he is currently a Professor. His principal area of research includes electrically small antennas for wireless communications, reader and tag antennas for RFID, on-glass and conformal antennas for vehicles and aircraft, and array antennas for GPS applications.

YONG BAE PARK received the B.S., M.S., and Ph.D. degrees in electrical engineering from the Korea Advanced Institute of Science and Technology, South Korea, in 1998, 2000, and 2003, respectively. From 2003 to 2006, he was with the Korea Telecom Laboratory, Seoul, South Korea. In 2006, he joined the School of Electrical and Computer Engineering, Ajou University, South Korea, where he is currently a Professor. His research interests include electromagnetic field analysis, metamaterial antennas, radomes, and stealth technology.